I-Q Mismatch Estimation and Compensation in Millimeter-Wave Wireless Systems

Yifan Zhu, Chris Hall and Akbar Sayeed
Department of Electrical and Computer Engineering
University of Wisconsin - Madison

***Abstract*—A salient feature of millimeter-wave (mmW) wireless systems is their large bandwidths. A direct consequence is that radio frequency (RF) non-idealities, such as phase noise, I-Q imbalance, and non-ideal frequency response of bandpass filters, become more pronounced compared to existing systems operating below 6 GHz. However, investigations of the impact of such non-idealities and techniques for their compensation are limited. In this paper, the problem of I-Q mismatch is investigated, motivated by the authors' recent work on mmW prototype design and development. First, a model for the non-ideal system is developed by modeling the in-phase (I) and quadrature (Q) passband channels separately, rather than the common complex baseband representation. The resulting channel matrix reveals the structure of interference introduced across I-Q channels and frequencies. Second, a new approach is developed for estimating the non-ideal channel using the new model. Third, a linear receiver architecture is developed to compensate for the interference caused by the I-Q mismatch. Finally, the performance of the new proposed system is compared to a baseline conventional system which ignores I-Q mismatch. The results indicate significant loss in performance even for modest values of I-Q mismatch parameters. In particular, the baseline system exhibits a saturation of output signal-to-interference-and-noise ratio (SINR) regardless of the input SNR. The new proposed system does not suffer from such saturation and its SINR can be increased indefinitely by increasing the input SNR. The analytical results are validated with experimental evaluation on a 28 GHz mmW wireless testbed.**

***Index Terms*—radio frequency non-idealities, wideband mixers, I-Q mismatch, millimeter-wave**

I. Introduction

Millimeter-wave (mmW) wireless systems are the focus of intense current research and development in industry and academia as part of fifth generation (5G) cellular and beyond. However, many technical issues need to be addressed to realize them in practice. One issue is the impact of the RF non-idealities that become more acute at the large (GHz) bandwidths in mmW systems. This issue is also important from the viewpoint of driving down the cost of mmW systems to accelerate large scale deployments. However, given the relatively nascent nature of mmW research and technology development, this issue has not been adequately addressed.

In this paper, the problem of I-Q mismatch in single input single output (SISO) mmW systems is investigated. First, a new system model is developed in Sec. III to capture I-Q mismatch at the transmitter (TX) and the receiver (RX) explicitly in terms of I and Q passband channels. The development yields a new baseband model for the channel matrix that can be decomposed into the component matrices reflecting the I-Q imbalance at the TX, RX and the phase offset between the TX/RX. The new matrix reveals the interference between I and Q channels and across frequencies and highlights the inadequacy of conventional channel estimation approaches that ignore mismatch. Using the new model, a new approach for channel estimation and equalization is proposed in Sec. IV to compensate for the mismatch. Simulation results are presented in Sec. V to illustrate the significant impact of I-Q mismatch on conventional receivers (SINR saturation and error floors) and the near-optimal performance of the new proposed approach. Experimental validation of the analytical results is provided through a 28 GHz mmW wireless testbed in Sec. VI.

This work is partly supported by the NSF under grants 1548996, 1703389 and 1629713 and the Wisconsin Alumni Research Foundation.

II. Related Work

The problem of I-Q imbalance has received extensive attention in recent years. All related existing works, that we have been able to find, can be placed in three categories. First, many works consider I-Q imbalance either at the TX or the RX [1]–[5]. In one of the earlier works [1], an equivalent baseaband model of I-Q imbalance at RX is developed that shows that imbalance introduces interference through the conjugate of the intended transmitted signal. This is a common feature confirmed and used by other works as well. In [3], I-Q imbalance and phase noise are studied and estimation and compensation methods similar to [1] are introduced. In [2], the results of [1] are extended to the multiuser scenario, and [4] studies the effect of I-Q imbalance and ADC (analog-to-digital converter) resolution in a multi-user MIMO scenario. The impact of I-Q imbalance at the TX for IEEE 802.11a/n/ac protocols is addressed in [5]. The paper also considers a timing skew between the I and Q channels.

The second catagory of existing works considers I-Q imbalance at both the TX and RX [6]–[13]. All of these works make different assumptions or approximations to obtain the final results, which are not always valid in practice. A general equivalent baseband model for the I-Q imbalance at the TX and RX is developed in the frequency domain in [6], and this model is used in many other works. Using the model, training signals for channel estimation and the corresponding method for estimating I-Q imbalance are developed. Under the assumption that the TX I-Q imbalance is relatively small, [6] is able to estimate the amplitude and phase imbalance parameters for both the TX and the RX. In [7], in addition

to the assumption of small I-Q imbalance at the TX, it is assumed that the frequency response of k_{th} sub-carrier is much larger than that for the $-k_{th}$ sub-carrier in an OFDM system. A low-IF (intermediate frequency) feedback architecture is proposed in [8] to achieve joint TX and RX I-Q imbalance compensation. Optimized estimation of the composite channel in the presence of I-Q imbalance is considered in [9], building on the equivalent baseband model in [6]. Frequency dependent I-Q imbalance at both TX and RX is addressed in [10], with the claim that the effect of I-Q imbalance at the TX and RX, and the impact of the channel, can be estimated separately under the assumption of small I-Q imbalance. The relationship between SINR and SNR is studied in [11] using the model in [6]. Two recent works focussing on I-Q imbalance estimation and compensation are [12], [13]. However, the method proposed in [12] makes a strong assumption that either the channel state information (CSI) is known or the ratio of I-Q imbalance effect at the TX and the RX is known. A compensation method is proposed in [13] based on an approximation of an equivalent baseband model of I-Q imbalance at both the TX and the RX, which is based on the small I-Q imbalance assumption.

The third category considers I-Q imbalance in specific applications such as mmW wireless, or uses different approaches for estimation and compensation such as on-chip calibration and maximum likelihood (ML) detection. In [14], the I-Q imbalance at both the TX and RX is studied for mmW communication, and joint estimation and compensation for single carrier frequency domain equalization (SC-FDE) systems is proposed. In order to separately estimate the channel and I-Q imbalance at the TX and RX, this paper defines a quantity called *channel variation energy*, which represents the smoothness of channel amplitude and is shown to be directly related to the I-Q imbalance effect. The authors are able to estimate the I-Q imbalance parameters by minimizing the channel variation energy. After the I-Q imbalance is estimated, the channel can be correctly estimated as well. A low-complexity method for on-chip self-calibration for I-Q imbalance is proposed in [15]. However, this method is off-line and cannot be used in real time. It is shown in [16] that I-Q imbalance can be exploited for diversity gain in an OFDM system.

To summarize, existing works on I-Q imbalance make strong assumptions that may not hold in practice. Furthermore, none of the works that we have discovered evaluate the methods in a real system. The results presented in this paper are not only new, they are also validated on an experimental 28 GHz mmW wireless testbed that we are being develoed at the Wireless Communication and Sensing Laboratory [17], [18]

III. System Model with I-Q Mismatch

In this section, we develop an I-Q imbalance model for a mmW system. The TX passpand signal is given by

$$x(t) = x_I(t)\cos(2\pi f_c t) + \alpha_T x_Q(t)\sin(2\pi f_c t + \phi_T) \quad (1)$$

where $x_I(t)$ and $x_Q(t)$ are the TX baseband signals, and (α_T, ϕ_T) are the amplitude and phase mismatch parameters of the TX mixer. At the RX, we apply a local oscillator (LO) with phase ϕ_o relative to TX LO. The I and Q signals at the output of the RX mixer are given by (before low-pass filtering)

$$\begin{aligned} y_I(t) &= x(t)\cos(2\pi f_c t + \phi_o) \\ y_Q(t) &= \alpha_R x(t)\sin(2\pi f_c t + \phi_o + \phi_R) \end{aligned} \quad (2)$$

where (α_R, ϕ_R) represent the IQ imbalance parameters of the RX mixer. Substituting $x(t)$ from (1) into (2), and ignoring the high frequency terms that are eliminated through low-pass filtering of (2), we get

$$\boldsymbol{y}(t) = \begin{bmatrix} y_I(t) \\ y_Q(t) \end{bmatrix} = \begin{bmatrix} H_{II} & H_{IQ} \\ H_{QI} & H_{QQ} \end{bmatrix} \begin{bmatrix} x_I(t) \\ x_Q(t) \end{bmatrix} = \boldsymbol{H}\boldsymbol{x}(t)$$

$$\begin{aligned} \boldsymbol{H} &= \begin{bmatrix} H_{II} & H_{IQ} \\ H_{QI} & H_{QQ} \end{bmatrix} \\ &= \begin{bmatrix} \cos(\phi_o) & \alpha_T \sin(\phi_T - \phi_o) \\ \alpha_R \sin(\phi_R + \phi_o) & \alpha_T\alpha_R \cos(\phi_o + \phi_R - \phi_T) \end{bmatrix} \end{aligned} \quad (3)$$

The matrix $\boldsymbol{H}$ can be decomposed into three matrices:

$$\begin{aligned} \boldsymbol{H} &= \begin{bmatrix} 1 & 0 \\ 0 & \alpha_R \end{bmatrix} \begin{bmatrix} 1 & 0 \\ \sin(\phi_R) & \cos(\phi_R) \end{bmatrix} \\ &\quad \times \begin{bmatrix} \cos(\phi_o) & -\sin(\phi_o) \\ \sin(\phi_o) & \cos(\phi_o) \end{bmatrix} \\ &\quad \times \begin{bmatrix} 1 & \sin(\phi_T) \\ 0 & \cos(\phi_T) \end{bmatrix} \begin{bmatrix} 1 & 0 \\ 0 & \alpha_T \end{bmatrix} \end{aligned} \quad (4)$$

where the first two matrices represent the mismatch effects at the RX, the third matrix represents the relative phase between the TX and RX, and the last two matrices represent the mismatch effect at the TX. The values for $\alpha_T, \alpha_R, \phi_T, \phi_R$ are constant over sufficiently long time scales (especially relative to the sampling interval in a mmW system which is typically on the order of a nanosecond) and thus can be measured or estimated. Note that in the absence of imbalance ($\alpha_T = \alpha_r = 1$, $\phi_T = \phi_R = 0$) and carrier offset $\phi_o = 0$, the channel matrix reduces to the identity matrix: $\boldsymbol{H} = \boldsymbol{I}$.

IV. Channel Estimation and Equalization that Accounts for Mismatch

In the absence of I-Q mismatch, the conventional approach to channel estimation and equalization is based on the complex baseband representation

$$y_c(t) = H_c x_c(t)\ ,\ H_c = H_I + jH_Q \quad (5)$$

$$x_c(t) = x_I(t) + jx_Q(t)\ ,\ y_c(t) = y_I(t) + jy_Q(t) \quad (6)$$

and estimation of the complex baseband channel coefficient H_c is simply based on the relation

$$\hat{H}_c = \frac{y_c(t)}{x_c(t)} \quad (7)$$

by transmitting known (complex) training signal $x_c(t)$ and measuring the corresponding received signal $y_c(t)$.

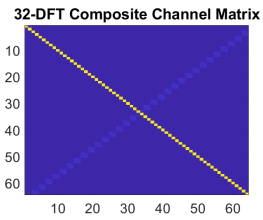

Fig. 1. An image of the channel matrix in the frequency domain (32-point OFDM). Amplitude mismatch = 0.5 dB. Phase mismatch = 2.5 deg.

In the presence of I-Q mismatch, the conventional approach is inadequate as evident from the non-diagonal structure of $\boldsymbol{H}$ in (4) and illustrated in Fig. 1 where an image of $\boldsymbol{H}$ is shown in the frequency (OFDM) domain for a system with mismatch at both the TX and the RX. There are two important things to note from Fig. 1: i) there are dominant entries in 2 $\times$ 2 blocks along the main diagonal (yellow squares) representing the coupling between the I and Q components, and ii) there are (weaker) non-zero block entries along the anti-diagonal representing coupling between positive and negative (baseband) frequencies. As we will see, these two characteristics of $\boldsymbol{H}$ make the conventional approach to channel estimation and equalization severely sub-optimal.

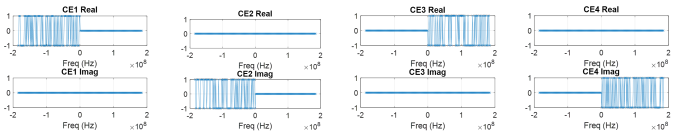

(a) (b) (c) (d)

Fig. 2. Training signals in the frequency (OFDM) domain for channel estimation in the proposed scheme. (a) Real part of lower half-band excited. (b) Imaginary part of lower half-band excited. (c) Real part of upper half-band excited. (d) Imaginary part of upper half-band excited.

Fig. 2 illustrates the OFDM training signal we propose for estimating the composite channel $\boldsymbol{H}$ in the presence of I-Q mismatch. Each plot shows the real part (top) and imaginary part (bottom) of the OFDM training symbols for the different tones. Given the structure of the composite channel matrix $\boldsymbol{H}$, illustrated in Fig. 1, the training signal consists of four OFDM packets shown in Fig. 2. The first two packets excite the real and imaginary parts of the lower half-band sequentially, as shown in Fig. 2(a)-(b). The third and fourth packets excite the real and imaginary parts of the upper half-band sequentially, as shown in Fig. 2(c)-(d). Using these training signals, the diagonal and anti-diagonal blocks of $\boldsymbol{H}$ (see Fig. 1) can be directly estimated. The rest of the entries of $\boldsymbol{H}$ are explicitly set to zero given the expected structure of $\boldsymbol{H}$. Once an estimate of $\boldsymbol{H}$ is available at the RX, a number of techniques can be used for equalizing the channel; e.g. linear zero-forcing or minimum-mean-squared error (MMSE) equalizers [19]. We illustrate the results for linear MMSE equalizers.

V. Performance Assessment

We now present initial numerical results to illustrate the significant impact of I-Q mismatch and the gains in performance due to the proposed compensation approach. Essentially, the presence of I-Q mismatch introduces interference between the I and Q channels (and positive and negative frequencies) that has to be estimated and then exploited for interference compensation at the RX. The performance of a conventional (complex baseband) approach to channel estimation and equalization that ignores I-Q mismatch is compared with the new proposed approach that accounts for the mismatch in both channel estimation and equalization, as outlined in Sec. IV.

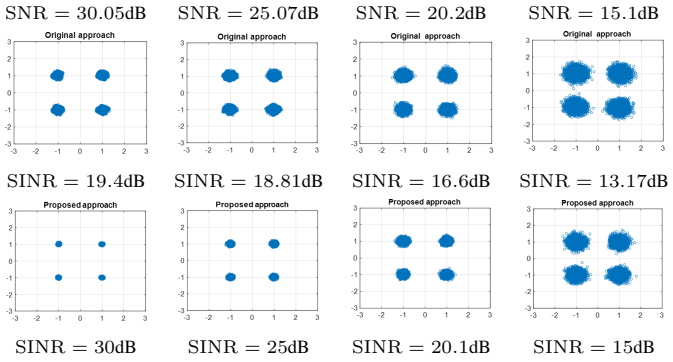

Fig. 3. Constellation comparison for QAM reception with the conventional complex-baseband model (top row) versus the new proposed model (bottom row) for four SNRs (left to right): 30.05dB, 25.07dB, 20.2dB, 15.1dB.

Fig. 3 compares the two approaches in terms of the received quadrature amplitude modulation (QAM) constellation symbols, transmitted using an OFDM packet with 256 tones. Perfect estimates of the effective channel matrix, which we refer to as channel state information (CSI), are assumed in both approaches and the results are shown for four different SNRs from left to right. The top row shows the constellations and the output SINRs for the conventional receiver, and the bottom row shows the constellations and SINRs for the new proposed approach. The amplitude mismatch is $20\log_{10}(\alpha_T/\alpha_R) = 0.5$dB and the phase mismatch is $\phi_T - \phi_R = 2.5$deg, reflecting the manufacturer's specifications for the I-Q mixers used in our mmW beamspace MIMO testbed [17], [18]. As evident, the new method yields a higher SINR (close to the SNR) compared to the conventional method.

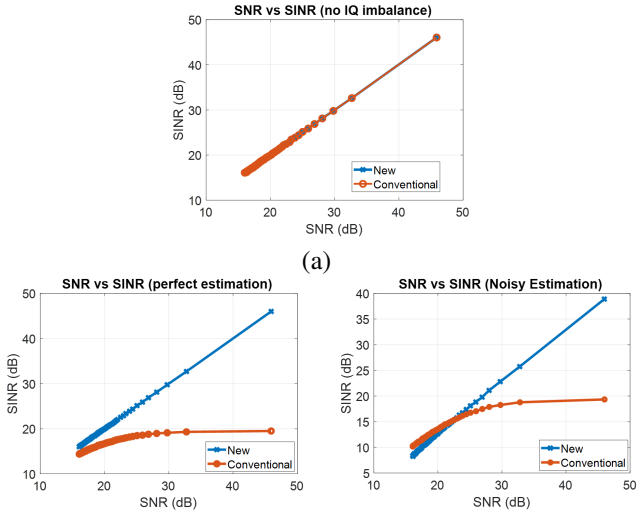

Fig. 4. SINR versus SNR comparison for: (a) perfect CSI and no imbalance, (b) perfect CSI with amplitude imbalance 0.5dB and phase imbalance 2.5deg, (c) noisy CSI with same I-Q imbalance as (b).

The behavior of SINR versus SNR is further explored in Fig. 4 starting with Fig. 4(a) which shows the performance of the two approaches for perfect CSI and no mismatch. As expected, both approaches yield identical SINR versus SNR performance with SINR = SNR. Fig. 4(b) compares the perfect CSI performance of the two approaches in the presence of I-Q mismatch (mismatch parameters the same as in Fig. 3). As evident, the conventional approach is interference limited since the output SINR saturates to a fixed value regardless of the SNR. On the other hand, the new approach is noise limited and the output SINR can be increased indefinitely by increasing SNR. Fig. 4(c) shows that for noisy CSI (estimation SNR the same as communication SNR), the conventional approach yields a higher SINR at low SNR values (due to the larger number of parameters to be estimated in the new approach), but the new approach eventually dominates for higher SNR values and without SINR saturation.

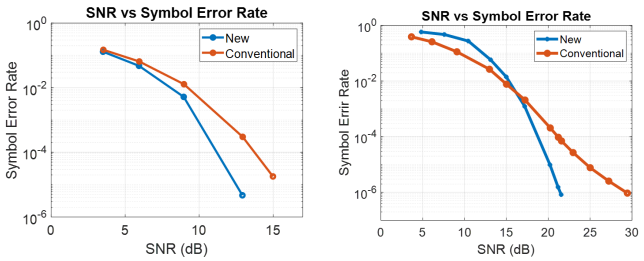

(a) (b)

Fig. 5. Symbol error rate (SER) versus SNR comparison for conventional and new approaches with amplitude imbalance of 1dB and phase imbalance of 5deg. (a) perfect CSI. (b) noisy CSI.

Finally, Fig. 5 compares the performance of the two approaches with perfect and noisy CSI for a larger mismatch: amplitude mismatch of 1dB and phase mismatch of 5deg. The figure compares the QAM symbol error rate (SER) for the two approaches with perfect CSI (a) and noisy CSI (b). As evident, the new approach always performs better than the conventional approach for perfect CSI, whereas it begins to dominate the conventional approach at sufficiently high SNR for noisy CSI. Note that the SER of the conventional approach will eventually exhibit an error floor for higher SNR (as can be seen in (b)) reflecting the behavior in Fig. 4(c).

VI. Experimental Evaluation on a 28 GHz Testbed

In this section, we evaluate the proposed I-Q estimation and compensation method using a 28 GHz mmW MIMO wireless testbed that we are developing [17], [18]. The experimental evaluation confirms the significant gains promised by the new method compared to the conventional approach. Two sets of results are presented: the first is based on a wired loopback measurement, and the second is based on over-the-air (OTA) wireless measurement. For details on the testbed specifications, the readers are referred to [17], [18].

A. Loopback Measurement

The loopback measurement set up is shown in Fig. 6. The output of the TX I-Q mixer is directly connected via a cable to the input of the RX I-Q mixer as illustrated in Fig. 6(a). The power amplifier (PA) at the TX and the low-noise amplifier (LNA) at the RX are not included in this measurement. Furthermore, to focus on the impact of I-Q mismatch, the local oscillators (LOs) for both the TX I-Q mixer and the RX I-Q mixer are driven by the same common reference source. Fig. 6(b) shows a picture of the actual hardware set up.

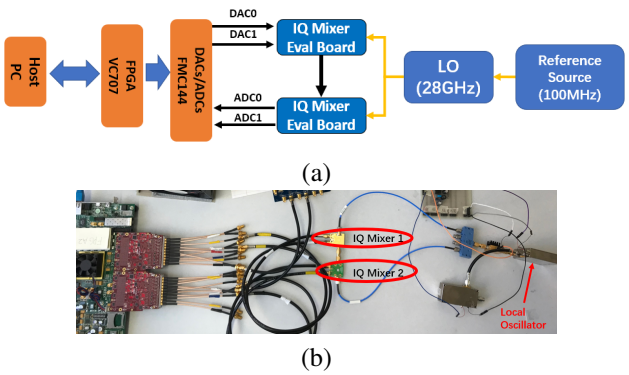

(a)

(b)

Fig. 6. Loopback measurement set up. (a) A schematic illustrating the loopback measurement. (b) The actual hardware set up.

The same type of I-Q mixer is used for up conversion at the TX and down conversion at the RX. The I-Q mixer used is HMC-1042L (Analog Devices) and has an amplitude imbalance of 0.5 dB and phase imbalance of 2.5 deg according to the manufacturer's specifications. A 16-bit signal from the DAC, with an amplitude of $0.5V_{pp}$, is fed to the TX I-Q mixer at a symbol rate of 370 MHz. The ADC captures the signal at the output of the RX I-Q mixer at a sampling rate of 370 MHz with 16-bit resolution. The maximum input voltage range for the ADC is $1.7V_{pp}$.

Transmit frames for the proposed method and the conventional method are shown in Fig. 7. Each frame consists of three blocks: frame synchronization (FS), channel estimation (CE), and data. The frames for both methods are identical except for the CE block. A 256-point OFDM modulation is used for both CE and data blocks. The FS block signal consists of a pseudo-random sequence for correlation-based time synchronization [17], [18] . The data block consists of four identical 256-point OFDM data sub-blocks, and each of them uses a subset of 175 sub-carriers for data transmission using a 4-QAM constellation.

Fig. 7(a) shows the frame signal for the proposed method; the CE block is as in Fig. 2. The four CE sub-blocks (1,2,3 and 4) in Fig. 7(a) correspond to the four OFDM packets ((a), (b), (c) and (d)) in Fig. 2. Within each CE block, the corresponding OFDM packet is repeated three times to improve the SNR in channel estimation through averaging. The frame signal for the conventional method is shown in Fig. 7(b). The CE block is repeated four times to improve the SNR. The conventional method uses a complex-valued chirp signal in the frequency domain for channel estimation as shown in Fig. 7 (c). In this case, both the real and imaginary parts for all sub-carriers are transmitted simultaneously (exploiting the orthogonality

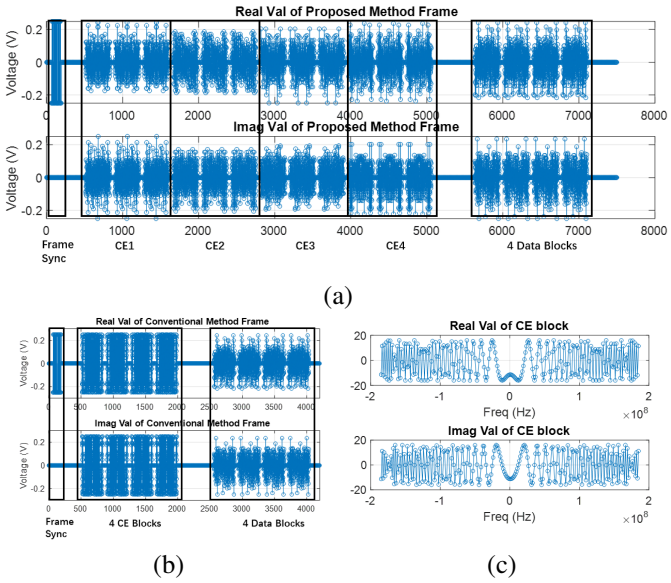

Fig. 7. Transmit frame structure in the time domain using 256-point OFDM packets for CE and data blocks. (a) Frame components for the proposed method. (b) Frame components for the conventional method. (c) CE training signal for the conventional method in the *frequency domain* (the CE training signal for the proposed method is illustrated in Fig. 2.)

between the different sub-carriers, and between the I and Q channels for each sub-carrier, in the absence of I-Q mismatch).

We note that for N-point OFDM modulation, the shortest training signal (without averaging) for the conventional method uses a single N-point OFDM packet. On the other hand, the shortest training signal for the proposed method uses four N-point OFDM packets (see Fig. 2).

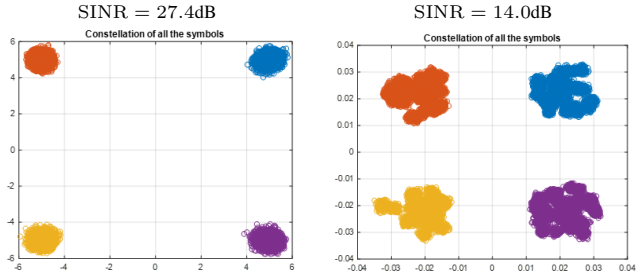

Fig. 8. Received I-Q data signals after equalization. The received signal SNR is 31.6dB. (a) proposed method. (b) conventional method.

Fig. 8 compares the performance of the proposed and conventional methods for 256-point OFDM signaling and plots the I-Q values of the equalized signal at the RX. The SNR of the received signal is around 31 dB. The received symbols show a tighter QAM constellation for the proposed method (Fig. 8(a)) and it is also reflected in the higher SINR of about 27 dB for the proposed method relative to the conventional method (Fig. 8(b)) that achieves an SINR of around 14dB. Thus, in the presence of relatively modest I-Q mismatch, the proposed method delivers an SINR gain of about 13dB compared to the conventional method. This is consistent with the SINR gain (at SNR $\approx$ 32dB) in the results in Fig. 4(b) .

We next estimate the full channel matrix $\boldsymbol{H}$ in the proposed method using a different 32-point OFDM frame shown in Fig. 9 in the time domain. Note that there are 64 sub-blocks

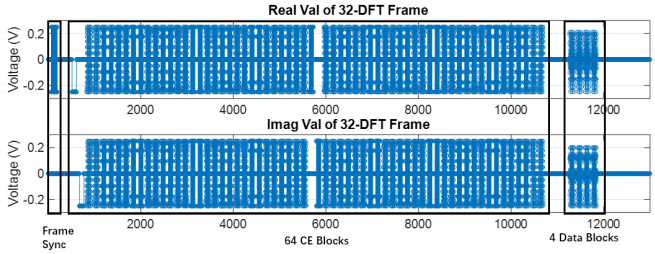

Fig. 9. 32-point OFDM frame in time domain for estimation of the full channel matrix $\boldsymbol{H}$.

(each corresponding to a 32-OFDM packet) in the CE block of the transmit frame. This is because for each 32-OFDM packet: i) only a single sub-carrier is excited, and ii) either I or Q channel of the sub-carrier is excited. That is, the I and Q channels of each sub-carrier are separately and sequentially excited using dedicated OFDM packets to estimate the full channel matrix $\boldsymbol{H}$, as shown in Fig. 10. Thus, for an N-OFDM packet, the CE block consists of 2N N-OFDM packets (in this case 64 32-OFDM packets). Out of the 32 OFDM carriers, only 22 sub-carriers are used for data and channel estimation.

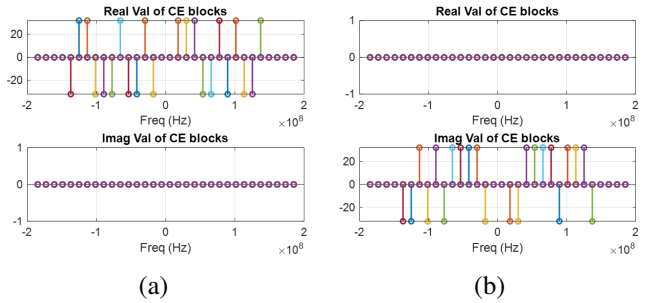

Fig. 10. Illustration of CE blocks in the frequency domain for full channel estimation. The I and Q channels for each sub-carrier are excited individually and sequentially over time, each using a dedicated OFDM packet. QAM symbols are used in the CE blocks and are superimposed for the 22 valid sub-carriers in the figure. (a) I-channel excitation. (b) Q-channel excitation.

For the 32-OFDM frame measurement, channel estimates are averaged over 5 frame captures (to improve SNR) since the channel is stable over a much longer duration in the loopback measurement. Fig. 11(a) shows the full channel matrix estimated using the 32-OFDM packets. The estimated channel matrix confirms the structure of $\boldsymbol{H}$ in the new model, shown in Fig. 1; the non-zero channel entries are concentrated on the diagonal and anti-diagonal blocks. Fig. 11(b) shows the equalized I-Q symbols at the receiver, using the full channel matrix, that correspond to a received SNR of about 33 dB and post-equalization SINR of about 29dB, which is again consistent with the results in Fig. 4.

B. Over-The-Air Wireless Measurement

For the wireless measurement, we add a power amplifier (PA) and a bandpass filter (BPF) to the TX, and a BPF and

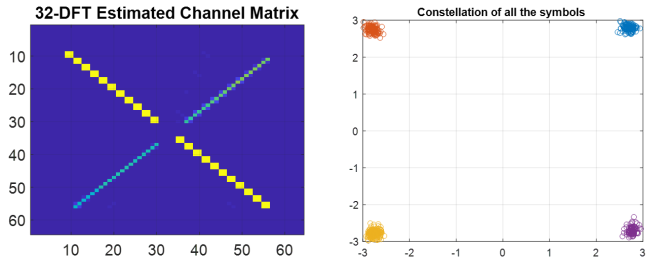

(a) (b)

Fig. 11. Results from 32-OFDM measurement. (a) Estimated full channel matrix. (b) RX I-Q data symbols: SNR = 33.11dB; SINR = 28.7dB.

a low noise amplifier (LNA) to the RX. The TX has a single waveguide antenna and its schematic and picture are shown in Fig. 12. The receiver schematic and picture are shown in Fig. 13. The RX has a 4×4 waveguide antenna array and four RF chains/channels are connected to the central four antennas.[1] The rest of the components and operational parameters are the same as in the loopback measurement. Again, to focus on the impact of I-Q mismatch, we drive both the TX and RX oscillators with a common reference source. The distance between the TX and RX is set to be about 4 inches to ensure a high-SNR measurement.[2]

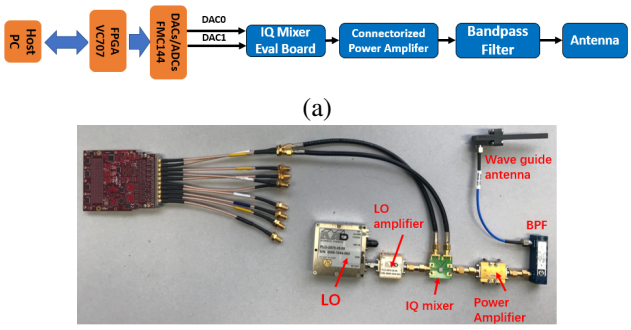

(a) (b)

Fig. 12. Single antenna TX set up for the wireless measurement. (a) TX schematic. (b) TX hardware.

For the wireless measurements, we again use the 256-OFDM frames shown in Fig. 7(a) and Fig. 7(b) for the proposed and conventional methods, respectively. Furthermore, 50 frame measurements are captured for each method. Fig. 14 shows the I-Q symbols for the equalized signals from the four antennas at the RX: (a) proposed method, and (b) conventional method. The SNRs and SINRs for the four antennas/channels are also shown. As can be seen, the received SNR is around 36-37 dB for both methods. The proposed method achieves an SINR around 25 dB, and conventional method achieves an SINR of around 16 dB. This indicates that I-Q mismatch cannot be ignored, and that the operational SINR can be increased by about 9-10 dB by using the proposed method, increasing the operational link length by a factor of about 3.

[1]The RX can also do hybrid beamforming by putting a mmW (dielectric) lens in front of the 4×4 waveguide array to create a lens array. [17], [18]

[2]The distance can be increased significantly when the RX operates with a 6" beamforming lens which has a gain of about 30dBi [18].

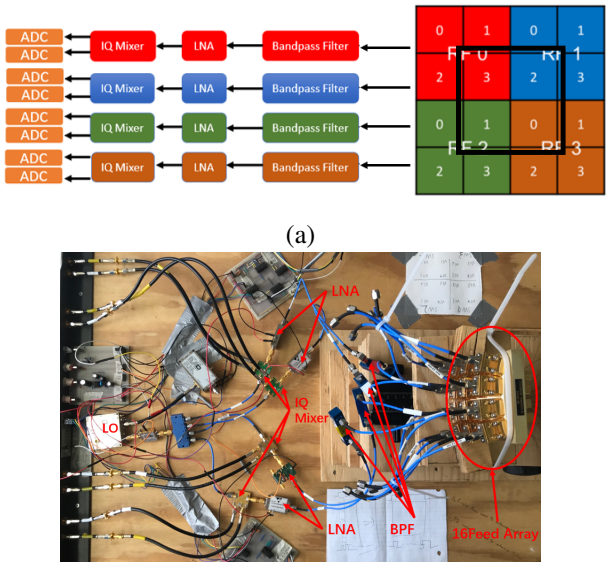

(a) (b)

Fig. 13. Four antenna RX set up for the wireless measurement. (a) RX schematic. (b) RX hardware set up for one RF chain. Measurements are made with four identical RF chains.

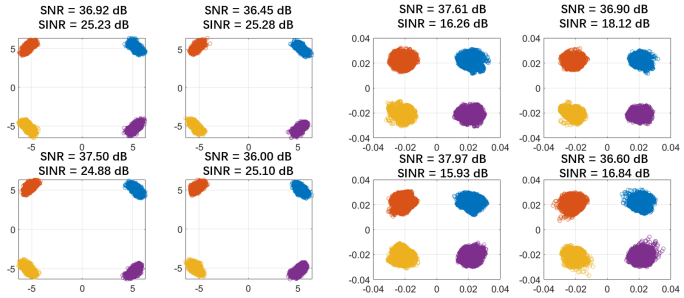

(a) (b)

Fig. 14. I-Q symbols for the equalized signals from the four antennas at the RX. (a) Proposed method. (b) Conventional method.

VII. Concluding Remarks

We have proposed a new approach to channel estimation and equalization in the presence of I-Q mismatch that is expected to be prevalent in emerging mmW wireless systems due to their large bandwidths. Our simulation and experimental results based on a 28 GHz testbed indicate that that the impact of I-Q mismatch is significant. While conventional methods exhibit an error floor (or SINR saturation), the new method for estimating and compensating I-Q imbalance promises significant performance gains without SINR saturation.

While the results are promising, we emphasize that these are only preliminary. In particular, the proposed method imposes a higher training and estimation overhead. Thus, we are investigation methods to reduce the overhead. One approach, if possible, is to reformulate the new channel model in complex baseband so that variants of conventional training and estimation techniques can be used. Another possibility is to directly estimate the mismatch parameters rather than the composite matrix $\boldsymbol{H}$.

REFERENCES

[1] J. Tubbax, B. Come, L. V. der Perre, S. Donnay, M. Engels, H. D. Man, and M. Moonen, "Compensation of IQ imbalance and phase noise in OFDM systems," *IEEE Transactions on Wireless Communications*, vol. 4, no. 3, pp. 872–877, May 2005.

[2] N. Kolomvakis, M. Matthaiou, and M. Coldrey, "IQ imbalance in multiuser systems: Channel estimation and compensation," *IEEE Transactions on Communications*, vol. 64, no. 7, pp. 3039–3051, July 2016.

[3] C.-J. Tsai, C.-H. Liao, and T.-D. Chiueh, "IQ imbalance and phase noise mitigation for wireless OFDM systems," in *2008 IEEE International Symposium on Circuits and Systems*, May 2008, pp. 2482–2485.

[4] S. Wang and L. Zhang, "Signal processing in massive MIMO with IQ imbalances and low-resolution ADCs," *IEEE Transactions on Wireless Communications*, vol. 15, no. 12, pp. 8298–8312, Dec 2016.

[5] M. Janaswamy, N. K. Chavali, and S. Batabyal, "Measurement of transmitter IQ parameters in HT and VHT wireless LAN systems," in *2016 International Conference on Signal Processing and Communications (SPCOM)*, June 2016, pp. 1–5.

[6] T. C. W. Schenk, P. F. M. Smulders, and E. R. Fledderus, "Estimation and compensation of TX and RX IQ imbalance in OFDM-based MIMO systems," in *2006 IEEE Radio and Wireless Symposium*, Jan 2006, pp. 215–218.

[7] I. T. Lu and J. Chang, "Joint transmitter and receiver IQ imbalance estimation and compensation for OFDM systems," in *2010 IEEE Radio and Wireless Symposium (RWS)*, Jan 2010, pp. 476–479.

[8] C. H. Peng, P. Liang, C. Chien, B. Narasimhan, and H. C. Hwang, "Joint TX/RX IQ mismatch compensation based on a low-IF internal feedback architecture," in *2012 IEEE Vehicular Technology Conference (VTC Fall)*, Sept 2012, pp. 1–5.

[9] W. Hou and M. Jiang, "Enhanced joint channel and IQ imbalance parameter estimation for mobile communications," *IEEE Communications Letters*, vol. 17, no. 7, pp. 1392–1395, July 2013.

[10] Y. Li, L. Fan, H. Lin, and M. Zhao, "A new method to simultaneously estimate TX/RX IQ imbalance and channel for OFDM systems," in *2013 IEEE International Conference on Communications (ICC)*, June 2013, pp. 4551–4555.

[11] O. Özdemir, R. Hamila, and N. Al-Dhahir, "Exact average OFDM subcarrier SINR analysis under joint transmit receive I/Q imbalance," *IEEE Transactions on Vehicular Technology*, vol. 63, no. 8, pp. 4125–4130, Oct 2014.

[12] W. Zhang, R. C. de Lamare, C. Pan, and M. Chen, "Joint TX/RX IQ imbalance parameter estimation using a generalized system model," in *2015 IEEE International Conference on Communications (ICC)*, June 2015, pp. 4704–4709.

[13] M. A. Ali, W. Kumar, and M. Arif, "OFDM receiver design in the presence of both Tx and Rx IQ imbalance over frequency selective channels," in *2016 IEEE Sixth International Conference on Communications and Electronics (ICCE)*, July 2016, pp. 94–98.

[14] X. Cheng, Z. Luo, and J. Liu, "Joint estimation and compensation of transmitter and receiver IQ imbalances in millimeter-wave SC-FDE systems," in *2015 IEEE International Conference on Communications (ICC)*, June 2015, pp. 1274–1279.

[15] C. Li, M. Li, S. Pollin, B. Debaillie, M. Verhelst, L. V. D. Perre, and R. Lauwereins, "Reduced complexity on-chip IQ-imbalance self-calibration," in *2012 IEEE Workshop on Signal Processing Systems*, Oct 2012, pp. 31–36.

[16] M. Marey, M. Samir, and M. H. Ahmed, "Joint estimation of transmitter and receiver IQ imbalance with ML detection for alamouti OFDM systems," *IEEE Transactions on Vehicular Technology*, vol. 62, no. 6, pp. 2847–2853, July 2013.

[17] J. Brady, J. Hogan, and A. Sayeed, "Multi-beam MIMO prototype for real-time multiuser communication at 28 GHz," *IEEE Globecom Workshop on Emerging Technologies for 5G*, Dec. 2016.

[18] A. Sayeed, C. Hall, and Y. Zhu, "A lens array multi-beam mimo testbed for real-time mmwave communication and sensing," *First Workshop on Millimeter-Wave Networks and Sensing Systems (Mobicom)*, October 2017.

[19] A. Sayeed and J. Brady, *Millimeter-Wave MIMO Transceivers: Theory, Design and Implementation*. Signal Processing for 5G: Algorithms and Implementations (F.-L. Luo and J. Zhang, Eds.), IEEE-Wiley, 2016.